Gauge invariant approach for supercooled phase transition from dark $U(1)_x$ hidden sectors involving sub-GeV dark matter

Wan-Zhe (Vic) FENG

Center for Joint Quantum Studies and Department of Physics, Tianjin University, PR. China

2025.9.27.

This talk is based on

WZF, Pran Nath "Cogenesis in a universe with vanishing $B-L$ within a gauged $U(1)_x$ extension", 1312.1334 [hep-ph].

WZF, Jinzheng Li, Zong-Huan Ye, Pran Nath, "Gravitational waves from cogenesis in a $B-L$ conserving Universe," 2510.xxxxx.

WZF, Zi-Hui Zhang, "Dark photon dark matter with *concrete* gravitational wave predictions", 2510.xxxxx.

Overview

Current dark matter status

- The non-observation of WIMPs has substantially challenged a large number of traditional dark matter models.
- Direct, indirect detections as well as collider constraints significantly narrow down the parameter space for the majority of WIMP dark matter candidates.
- $\Omega h^2 = 0.12$ now becomes a constraint to the dark matter models rather than an ultimate goal to achieve (for model builders).

Nightmare direct detection constraints on WIMPs

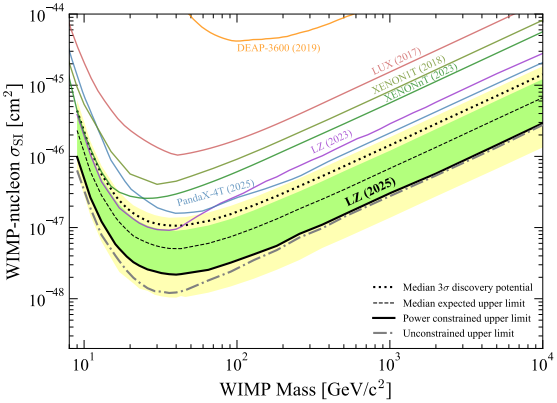

[LZ, 2025]

Dark matter detections

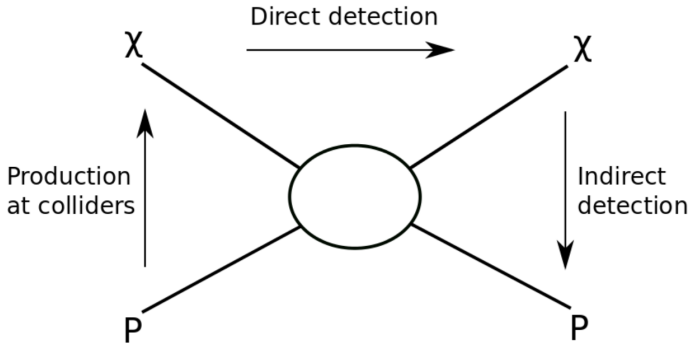

Freeze-out mechanism sets the coupling between WIMP and SM, which must inevitably be large. This leads to substantial elastic scattering cross-sections between WIMP and hadrons which have been already excluded by DM direct detections.

Post-WIMP era

- Sub-GeV dark matter: lack of direct detection experiments for this mass range (experimental constraints not that strong), MeV-WIMP freeze-out cross-sections require weaker couplings (lower than the current experimental constraints) with the SM particles compared with the traditional $\mathcal{O}(100)$ GeV WIMPs, some of the $3 \to 2$ annihilation freeze-out dark matter models prefer a MeV mass range...
- Quark-phobic type of models: dark matter does not directly annihilate to quarks, which seems rather unnatural, at least for me.
- Resonance models (remain subject to strong constraints from colliders). In many cases, DM and mediators are all pushed to $\mathcal{O}$(TeV) or above.
- Right-handed neutrino portal dark matter, somehow lack of (traditional) direct detection detectability due to dark matter does not interact with quarks.
- What about the $1 - 200$ GeV traditional WIMP models?
- Shall we completely abandon these models? What should we do now?

Explore more possibilities beyond the SM

- In the absence of experimental clues, we should broaden our exploration beyond the Standard Model, including the interplay of multiple hidden sectors, gravitational wave production, and new mechanisms or detectable phenomena within hidden sector(s).
- It is widely accepted that dark matter resides in one or multiple hidden sectors. Since dark matter hasn't been detected other than gravitational observations, it is possible that dark matter undergoes strong interactions across multiple hidden sectors, while only ultraweakly coupled to the Standard Model.

Multiple hidden sectors beyond the SM

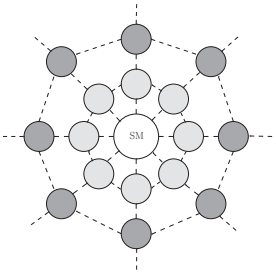

The Standard Model is in general directly or indirectly connected with multiple hidden sectors, with either weak scale coupling or ultraweak coupling. A hidden sector feebly interacted with the SM will evolve almost independently with respect to the observed Universe, and it possesses its own temperature.

Among hidden sectors, however, they may exhibit rather strong interactions.

Exploring deeper into multiple hidden sectors

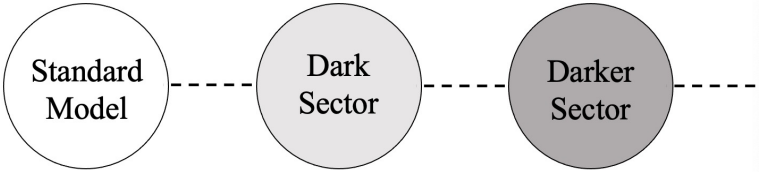

A graphic illustration of a darker sector which indirectly connected to the SM.

Connection of the dark sector with the SM: SUSY portal, Higgs portal, axion portal, fermion portal, right-handed neutrino portal, ($U(1)$) vector portal, gravity portal.

Connection of the darker sectors can be also through these portals, but with less experimental constraints.

Freeze-out WIMPs are facing stringent experimental constraints

- Dark matter candidates from a single dark sector through portal interactions are now subject to stringent experimental constraints (on masses and couplings for both dark matter candidates and mediators), e.g.,
  Higgs portal, axion portal, fermion portal, vector portal...

Freeze-out WIMPs are facing stringent experimental constraints

- Dark matter candidates from a single dark sector through portal interactions are now subject to stringent experimental constraints (on masses and couplings for both dark matter candidates and mediators), e.g.,
  Higgs portal, axion portal, fermion portal, vector portal...
- A fair conclusion: with the current sensitivities of both DM detectors and colliders, the usual WIMP dark matter candidates, which are subject to DM direct detection constraints (usually more important), cannot sufficiently annihilate into SM particles and will result in an overproduction of the relic dark matter through freeze-out.

Freeze-out WIMPs are facing stringent experimental constraints

- Dark matter candidates from a single dark sector through portal interactions are now subject to stringent experimental constraints (on masses and couplings for both dark matter candidates and mediators), e.g.,
  Higgs portal, axion portal, fermion portal, vector portal...
- A fair conclusion: with the current sensitivities of both DM detectors and colliders, the usual WIMP dark matter candidates, which are subject to DM direct detection constraints (usually more important), cannot sufficiently annihilate into SM particles and will result in an overproduction of the relic dark matter through freeze-out.
- This problem can be resolved with the assistant of additional darker sector [WZF, Zhang, 2024]: *annihilating to the darker*.

Annihilating to the darker

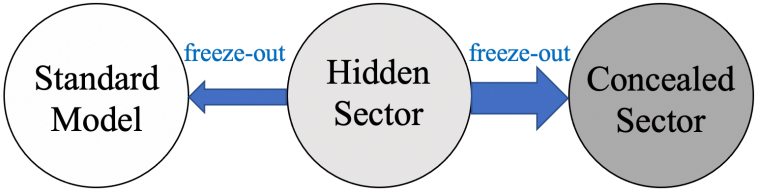

WZF, Zhang, "*Annihilating to the darker: a cure for WIMP,*" 2409.17217.

In addition to freezing out into the SM with only a small fraction (which may still provide direct detection signals for future experiments), the thermal WIMP χ_x $(1 - 200$ GeV) predominantly annihilate into a darker concealed sector.

Annihilating to the darker

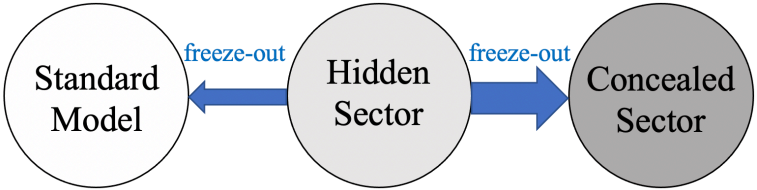

WZF, Zhang, "*Annihilating to the darker: a cure for WIMP,*" 2409.17217.

In addition to freezing out into the SM with only a small fraction (which may still provide direct detection signals for future experiments), the thermal WIMP χ_x $(1 - 200$ GeV) predominantly annihilate into a darker concealed sector. The connections can be any portal interactions.

An illustration: a simple two-$U(1)$ model

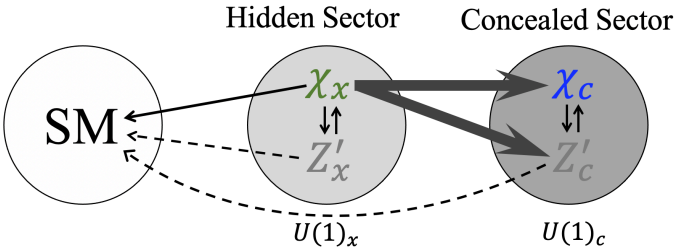

WZF, Zhang, "*Annihilating to the darker: a cure for WIMP,*" 2409.17217.

Case 1: The WIMP annihilates efficiently and achieves the observed relic density with the assistance of the concealed sector.
Case 2: The WIMP transforms into another type of dark matter within the concealed sector and attains the observed relic density.

Dark photon dark matter from $U(1)$ mixings

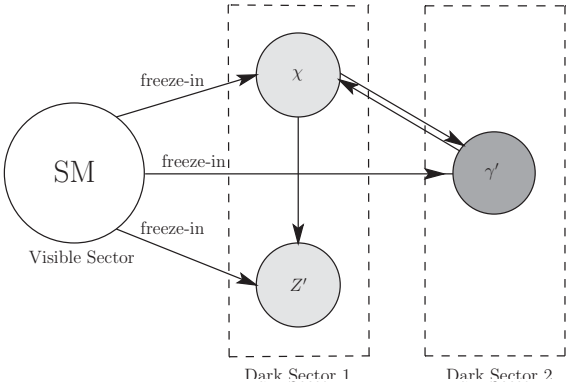

[Aboubrahim, WZF, Nath, Wang, 2103.15769]: dark photon dark matter from two $U(1)$'s can occupy almost 100% of the relic density.

A two-step freeze-in $U(1)$ model

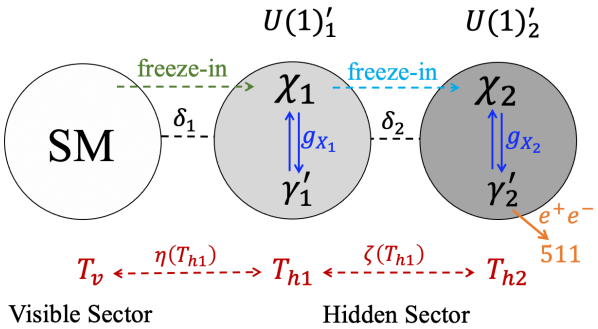

[WZF, Zhang, 2405.19431]: a hidden sector produced through the freeze-in mechanism, can further generate an even more hidden sector via an additional freeze-in process. Such a two-step freeze-in process produces dark matter coupled weaker-than-ultraweakly to the standard model particles, and is thus referred to as the "darker matter".

Cosmic coincidence

- Puzzle 1: The nature of dark matter.
- Puzzle 2: The origin of baryon asymmetry.

Cosmic coincidence

- Puzzle 1: The nature of dark matter.
- Puzzle 2: The origin of baryon asymmetry.
- Puzzle 3 (or maybe not): The cosmological abundances of dark and visible matter are comparable in magnitude $\Omega_{\rm DM}h_0^2/\Omega_{\rm B}h_0^2 \approx 5.5$.

Cosmic coincidence

- Puzzle 1: The nature of dark matter.
- Puzzle 2: The origin of baryon asymmetry.
- Puzzle 3 (or maybe not): The cosmological abundances of dark and visible matter are comparable in magnitude $\Omega_{\rm DM}h_0^2/\Omega_{\rm B}h_0^2 \approx 5.5$.

The similarity between $\Omega_{\rm DM}h_0^2$ and $\Omega_{\rm B}h_0^2$ suggests that the baryon asymmetry and dark matter abundance may share a common origin.

Baryon asymmetry

One proposed explanation for the comparable abundances of dark and visible matter is the asymmetric dark matter hypothesis [Kaplan, Luty, and Zurek, 2009]. In this framework, dark sector particles were in thermal equilibrium with the visible sector in the early universe, and thus their chemical potentials – quantifying the particle asymmetries – are naturally of the same order.

Baryon asymmetry

One proposed explanation for the comparable abundances of dark and visible matter is the asymmetric dark matter hypothesis [Kaplan, Luty, and Zurek, 2009]. In this framework, dark sector particles were in thermal equilibrium with the visible sector in the early universe, and thus their chemical potentials – quantifying the particle asymmetries – are naturally of the same order. If the dark-matter mass is of the same order as the baryon mass, the observed dark-to-baryon ratio can be naturally explained.

Baryon asymmetry

One proposed explanation for the comparable abundances of dark and visible matter is the asymmetric dark matter hypothesis [Kaplan, Luty, and Zurek, 2009]. In this framework, dark sector particles were in thermal equilibrium with the visible sector in the early universe, and thus their chemical potentials – quantifying the particle asymmetries – are naturally of the same order. If the dark-matter mass is of the same order as the baryon mass, the observed dark-to-baryon ratio can be naturally explained.

The observed ratio of dark to baryonic matter $\Omega_{\rm DM}/\Omega_{\rm B} \approx 5.5$, can then be reproduced by imposing a suitable constraint on the dark-matter mass. Defining B to be the total baryon number in the Universe and X to be the total dark matter number,

$$\frac{\Omega_{\rm DM}}{\Omega_{\rm matter}} = \frac{X \cdot m_{\rm DM}}{B \cdot m_{\rm B}} \approx 5\,,$$

the dark particle mass is given by

$$m_{\rm DM} \approx 5 \cdot \frac{B}{X} \cdot 1\,{\rm GeV}\,.$$

Asymmetry transfer interaction

- More specifically, the asymmetry can transfer from the visible sector to the dark sector via the asymmetry transfer interaction

$$\mathcal{L}_{\rm asy} = \frac{1}{M^n_{\rm asy}} \mathcal{O}_{\rm DM} \mathcal{O}_{\rm asy} \,,$$

  where $M_{\rm asy}$ is the scale of the interaction, $\mathcal{O}_{\rm asy}$ denotes an operator built from visible-sector fields that carries a nonvanishing $B-L$ quantum number, while $\mathcal{O}_{\rm DM}$ carries the opposite $B-L$ charge.
- This interaction decouples at a temperature higher than the dark matter mass. As the Universe cools, the dark matter asymmetry freezes at a level comparable to the baryon asymmetry, thereby explaining the observed relation between baryonic and dark matter abundances
- The original proposal assumes a preexisting baryon or lepton asymmetry, which is subsequently transferred to the dark sector [WZF, Nath, Peim, 2012, and many]. A direct generalization is the reverse scenario: the asymmetry is first generated in the dark sector and then transferred to the visible [WZF, Mazumdar, Nath, 2013, and many].

Generalization of the asymmetry transfer interaction

Beyond simple transfer mechanisms, a more general UV completion is provided by cogenesis scenarios, wherein the dark-matter and baryonic asymmetries are simultaneously generated from a common source [Davoudiasl, Morrissey, Sigurdson, Tulin, 2009; Gu, Lindner, Sarkar Zhang, 2010].

Generalization of the asymmetry transfer interaction

Beyond simple transfer mechanisms, a more general UV completion is provided by cogenesis scenarios, wherein the dark-matter and baryonic asymmetries are simultaneously generated from a common source [Davoudiasl, Morrissey, Sigurdson, Tulin, 2009; Gu, Lindner, Sarkar Zhang, 2010]. It is not easy:

- If the asymmetry is generated through the decay of the same Majorana fermions, there is no guarantee that the resulting visible and dark sector asymmetries will be equal [Falkowski, Ruderman, Volansky, 2011]. Consequently, the dark-to-baryon abundance ratio and the dark matter mass are no longer directly correlated, unless one invokes a mirror world scenario [An, Chen, Mohapatra Zhang, 2009; WZF, Yu, 2020].

Generalization of the asymmetry transfer interaction

Beyond simple transfer mechanisms, a more general UV completion is provided by cogenesis scenarios, wherein the dark-matter and baryonic asymmetries are simultaneously generated from a common source [Davoudiasl, Morrissey, Sigurdson, Tulin, 2009; Gu, Lindner, Sarkar Zhang, 2010]. It is not easy:

- If the asymmetry is generated through the decay of the same Majorana fermions, there is no guarantee that the resulting visible and dark sector asymmetries will be equal [Falkowski, Ruderman, Volansky, 2011]. Consequently, the dark-to-baryon abundance ratio and the dark matter mass are no longer directly correlated, unless one invokes a mirror world scenario [An, Chen, Mohapatra Zhang, 2009; WZF, Yu, 2020].
- The Standard Model operators available for asymmetry transfer are rather limited: $LH, LLe^c, LQd^c, u^c d^c d^c$. LH coupling has been extensively studied in the context of the seesaw. However, the seesaw mechanism intrinsically violates $B - L$

Generalization of the asymmetry transfer interaction

Beyond simple transfer mechanisms, a more general UV completion is provided by cogenesis scenarios, wherein the dark-matter and baryonic asymmetries are simultaneously generated from a common source [Davoudiasl, Morrissey, Sigurdson, Tulin, 2009; Gu, Lindner, Sarkar Zhang, 2010]. It is not easy:

- If the asymmetry is generated through the decay of the same Majorana fermions, there is no guarantee that the resulting visible and dark sector asymmetries will be equal [Falkowski, Ruderman, Volansky, 2011]. Consequently, the dark-to-baryon abundance ratio and the dark matter mass are no longer directly correlated, unless one invokes a mirror world scenario [An, Chen, Mohapatra Zhang, 2009; WZF, Yu, 2020].
- The Standard Model operators available for asymmetry transfer are rather limited: $LH, LLe^c, LQd^c, u^cd^cd^c$. LH coupling has been extensively studied in the context of the seesaw. However, the seesaw mechanism intrinsically violates $B - L$ and the RH neutrino acting as a visible-dark portal, may wash out the generated asymmetry.

Generalization of the asymmetry transfer interaction

Beyond simple transfer mechanisms, a more general UV completion is provided by cogenesis scenarios, wherein the dark-matter and baryonic asymmetries are simultaneously generated from a common source [Davoudiasl, Morrissey, Sigurdson, Tulin, 2009; Gu, Lindner, Sarkar Zhang, 2010]. It is not easy:

- If the asymmetry is generated through the decay of the same Majorana fermions, there is no guarantee that the resulting visible and dark sector asymmetries will be equal [Falkowski, Ruderman, Volansky, 2011]. Consequently, the dark-to-baryon abundance ratio and the dark matter mass are no longer directly correlated, unless one invokes a mirror world scenario [An, Chen, Mohapatra Zhang, 2009; WZF, Yu, 2020].
- The Standard Model operators available for asymmetry transfer are rather limited: $LH, LLe^c, LQd^c, u^cd^cd^c$. LH coupling has been extensively studied in the context of the seesaw. However, the seesaw mechanism intrinsically violates $B - L$ and the RH neutrino acting as a visible-dark portal, may wash out the generated asymmetry.
- Asymmetric operators other than LH already appear at mass dimension six. A consistent UV completion therefore naturally requires the introduction of new colored scalar states, or else necessitates a supersymmetric framework.

Cogenesis in a $B-L$ conserving Universe

With the following quantum numbers assignments:

	L	H	N	ψ	ϕ	X	X'	Φ_x
L No.	$+1$	0	0	$+1$	-1	$+\frac{1}{2}$	$+\frac{1}{2}$	0
$B-L$	-1	0	0	-1	$+1$	$-\frac{1}{2}$	$-\frac{1}{2}$	0
$U(1)_x$	0	0	0	0	0	$+1$	-1	$+1$

The complete Lagrangian of the model is given by

$$\begin{aligned}\mathcal{L} = \mathcal{L}_{\rm SM} &+ \lambda_i \overline{N_i}\psi\phi + y_i^{\psi}\overline{\psi}L_i H + y_x \phi \overline{X^c} X' + h.c. + \tfrac{1}{2}\overline{N_i}(\mathrm{i}\partial\!\!\!/ - M_i)N_i \\ &+ \overline{\psi}\mathrm{i}\partial\!\!\!/\psi - m_\psi\overline{\psi}\psi + |\partial_\mu\phi|^2 - m_\phi^2\phi^*\phi + \overline{X}(\mathrm{i}\partial\!\!\!/ - m_{\rm DM})X + \overline{X'}(\mathrm{i}\partial\!\!\!/ - m_{\rm DM})X' \\ &- \tfrac{1}{4}F_{x\,\mu\nu}F_x^{\mu\nu} - \tfrac{\epsilon}{2}F_{x\,\mu\nu}F^{\mu\nu} + |D_\mu\Phi_x|^2 - V_{\rm eff}(\Phi_x)\,.\end{aligned}$$

Cogenesis, DM secluded annihilation, Gravitational waves.

Perfectly bypass the first Sakharov condition

The basic ingredients necessary for baryogenesis are well known and consist of three Sakharov conditions [Sakharov, 1967]:

- The existence of baryon (or lepton) number violation
- the presence of C and CP violating interactions and
- out of equilibrium processes.

Full Boltzmann equation involving washout

The evolution of N_1 and the created net lepton number L, which is equal to the net Ψ number generated ($Y_L = Y_\Psi$), are governed by the following set of Boltzmann equations

$$\begin{aligned}
\frac{\mathrm{d}Y_{N_1}}{\mathrm{d}T} &= \frac{1}{T\bar{H}}\left[\langle\Gamma_{N_1}\rangle\left(Y_{N_1}-Y_{N_1}^{\mathrm{EQ}}\right)-\epsilon_L\langle\Gamma_{N_1}\rangle Y_{N_1}^{EQ}\times\frac{4\pi^2 g_{*S}Y_L}{15}\right] \\
&\quad+\frac{2s}{T\bar{H}}\left(\langle\sigma v\rangle_{N_1N_1\to\phi\bar{\phi}}+\langle\sigma v\rangle_{N_1N_1\to\psi\bar{\psi}}\right)\left(Y_{N_1}Y_{N_1}-Y_{N_1}^{\mathrm{EQ}}Y_{N_1}^{\mathrm{EQ}}\right), \\
\frac{\mathrm{d}Y_L}{\mathrm{d}T} &= -\frac{1}{T\bar{H}}\left(\epsilon_L\langle\Gamma_{N_1}\rangle\left(Y_{N_1}-Y_{N_1}^{\mathrm{EQ}}\right)-\frac{4\pi^2 g_{*S}Y_L}{15}\langle\Gamma_{N_1}\rangle Y_{N_1}^{\mathrm{EQ}}\right) \\
&\quad+\frac{s}{T\bar{H}}\frac{4\pi^2 g_{*S}Y_L}{15}\left(8\langle\sigma v\rangle_{\psi\psi\to\overline{\phi\phi}}^{\mathrm{RIS}}n_\psi^{\mathrm{EQ}}n_\psi^{\mathrm{EQ}}+4\langle\sigma v\rangle_{\psi\phi\to\overline{\psi\phi}}^{\mathrm{RIS}}n_\psi^{\mathrm{EQ}}n_\phi^{\mathrm{EQ}}\right).
\end{aligned}$$

where $s = 2\pi^2 h_{\mathrm{eff}}T^3/45$ and

$$\bar{H} = \frac{H}{1+\frac{1}{3}\frac{T}{h_{\mathrm{eff}}}\frac{\mathrm{d}h_{\mathrm{eff}}}{\mathrm{d}T}} = \sqrt{\frac{\pi^2 g_{\mathrm{eff}}}{90}}\frac{T^2/M_{\mathrm{Pl}}}{1+\frac{1}{3}\frac{T}{h_{\mathrm{eff}}}\frac{\mathrm{d}h_{\mathrm{eff}}}{\mathrm{d}T}}.$$

The mass and mixing in the observed neutrino sector

The observed tiny neutrino mass is explained by introducing three right-handed Dirac neutrinos with the Yukawa interactions and the full mass terms in the neutrino sector can be written as

$$\mathcal{L}_\nu^{\rm mass} = -y_{ij}^\nu \overline{\nu_{j\,R}} L_i H - y_i^\psi \overline{\psi_R} L_i H - \mu_i \overline{\nu_{i\,R}} \psi_L + h.c. - m\overline{\psi}\psi\,,$$

which generate the neutrino mass terms

$$\begin{aligned}\mathcal{L}_\nu^{\rm mass} = &-m_{ij}^\nu (\overline{\nu_{i\,L}}\nu_{j\,R} + \overline{\nu_{j\,R}}\nu_{i\,L}) - m_i^\psi (\overline{\psi_R}\nu_{i\,L} + \overline{\nu_{i\,L}}\psi_R) \\ &- \mu_i (\overline{\psi_L}\nu_{i\,R} + \overline{\nu_{i\,R}}\psi_L) - m_\psi (\overline{\psi_R}\psi_L + \overline{\psi_L}\psi_R)\,,\end{aligned}$$

where $m_{ij}^\nu = \frac{1}{\sqrt{2}} y_{ij}^\nu v_{\rm SM}$, $m_i^\psi = \frac{1}{\sqrt{2}} y_i^\psi v_{\rm SM}$, and can be rewritten in the matrix form

$$\mathcal{L}_\nu^{\rm mass} = -\begin{pmatrix} \overline{\nu_{e\,L}} & \overline{\nu_{\mu\,L}} & \overline{\nu_{\tau\,L}} & \overline{\psi_L} \end{pmatrix} \begin{pmatrix} m_{ee}^\nu & m_{e\mu}^\nu & m_{e\tau}^\nu & \mu_e \\ m_{\mu e}^\nu & m_{\mu\mu}^\nu & m_{\mu\tau}^\nu & \mu_\mu \\ m_{\tau e}^\nu & m_{\tau\mu}^\nu & m_{\tau\tau}^\nu & \mu_\tau \\ m_e^\psi & m_\mu^\psi & m_\tau^\psi & m_\psi \end{pmatrix} \begin{pmatrix} \nu_{e\,R} \\ \nu_{\mu\,R} \\ \nu_{\tau\,R} \\ \psi_R \end{pmatrix} + h.c.\,.$$

The observed neutrino mixings

A 4×4 unitary matrix U transforms the neutrino flavor eigenbasis to mass eigenbasis, and the top-left 3×3 block of the rotation matrix U should match the PMNS matrix obtained through experimentation. Other neutrino experimental constraints include: (1) the upper bound of neutrino mass sum, (2) the experimental fitting values of the mass-square differences (3) non-unitarity constraint, which sets limits on the size of the mixing between the SM neutrinos and the massive fermion ψ (4) the measured Dirac phase. We found the 4×4 neutrino mass matrix taking the following form can do the job:

$$\begin{pmatrix} m^{\nu}_{ee} & 0 & 0 & \mu_e \\ 0 & m^{\nu}_{\mu\mu} & 0 & \mu_\mu \\ 0 & 0 & m^{\nu}_{\tau\tau} & \mu_\tau \\ m^{\psi}_{e} & m^{\psi}_{\mu} & m^{\psi}_{\tau} & m_\psi \end{pmatrix},$$

which is remarkable in that the three SM neutrino flavors initially exhibit no mixing in the upper-left 3×3 block of the mass matrix, and all observed mixing arises solely from the presence of the new particle ψ.

Dark matter annihilation

In the model there are two dark matter candidates X, X' which are produced equally from the decay of the heavy ϕ particle. The asymmetric component of X, X' constitutes the dominant contribution to the total dark matter relic abundance. Using Eqs. (**??**) and (**??**), one finds

$$m_{\rm DM} = 5.5 \times \frac{30}{97} \times \frac{1}{2} \approx 0.85\,{\rm GeV}\,,$$

where the $1/2$ factor arises because both X, X' carry a $B-L$ number $-1/2$.
The symmetric component of X, X' can be efficiently reduced from the annihilation processes

$$\overline{X}X \to A_x A_x\,, \qquad \overline{X'}X' \to A_x A_x\,,$$

into sub-GeV $U(1)_x$ dark photons A_x.

Evolution of the asymmetric dark matter

The Boltzmann equations govern the evolution of the dark matter particle X is given by (X' constitutes the other half of the dark matter relic density and the computation of X' evolution is similar)

$$\begin{aligned}
\frac{\mathrm{d}Y_X}{\mathrm{d}T} &= \frac{s}{T\bar{H}}\left(Y_X Y_{\overline{X}}\langle\sigma v\rangle_{\overline{X}X\to A_x A_x} - Y_{A_x}^2\langle\sigma v\rangle_{A_x A_x\to\overline{X}X}\right)\\
\frac{\mathrm{d}Y_{\overline{X}}}{\mathrm{d}T} &= \frac{s}{T\bar{H}}\left(Y_X Y_{\overline{X}}\langle\sigma v\rangle_{\overline{X}X\to A_x A_x} - Y_{A_x}^2\langle\sigma v\rangle_{A_x A_x\to\overline{X}X}\right)\\
\frac{\mathrm{d}Y_{A_x}}{\mathrm{d}T} &= \frac{s}{T\bar{H}}\Big(2Y_{A_x}^2\langle\sigma v\rangle_{A_x A_x\to\overline{X}X} - 2Y_X Y_{\overline{X}}\langle\sigma v\rangle_{\overline{X}X\to A_x A_x}\\
&\qquad + \frac{1}{s}\langle\Gamma\rangle_{A_x\to\overline{f}f} + Y_f Y_{\bar{f}}\langle\sigma v\rangle_{\overline{f}f\to A_x}\Big)
\end{aligned}$$

where

$$Y_X - Y_{\overline{X}} = Y_L \simeq 3\times 10^{-10}\,,$$

determined by the cogenesis.

Evolution of the asymmetric dark matter

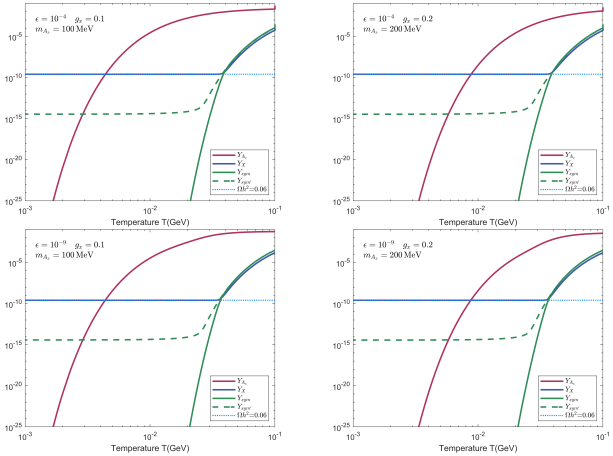

Figure: Thermal evolution of $Y_{A_x}, Y_X, Y_{sym}, Y_{sym'}$ for four benchmark models.

Dark photon constraints from dark matter secluded annihilation

We compute the minimal $U(1)_x$ gauge coupling that yields a sufficient annihilation of the symmetric dark matter component, so that the constraint $\Omega_{sym}h^2 \lesssim 1\% \times 0.12$, for dark photon masses in the range 20 MeV $-$ 1 GeV is satisfied.

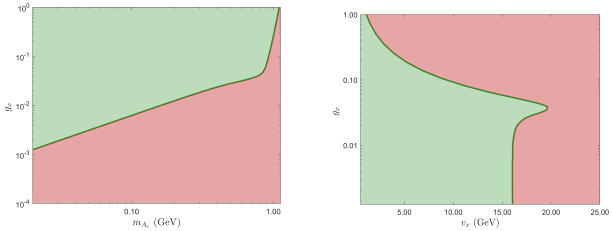

Figure: Left panel: g_x versus the dark photon mass; right panel: g_x versus the $U(1)_x$ vacuum expectation value v_x. The shaded light-green regions in both panels indicate the parameter space of g_x that yields sufficient secluded annihilation of the symmetric dark matter component, for dark photon masses in the range 20 MeV $-$ 1 GeV. The kinetic mixing between $U(1)_x$ and the hypercharge gauge field is fixed at $\epsilon = 10^{-4}$, consistent with current experimental constraints.

Characteristic temperatures

- Critical temperature T_c: two zero minima of V_{eff} are generated.
- Nucleation temperature T_n: true vacuum bubbles start to nucleate and the phase transition occurs. T_n is estimated when one bubble is nucleated in a Hubble volume

$$\int_0^{t_n} \Gamma/H^{-3}\mathrm{d}t \simeq 1\,,$$

  where $\Gamma = \mathcal{A}(T)\mathrm{e}^{-S_3(T)/T}$ denotes the bubble nucleation rate. For the electroweak phase transition, T_n can be well-approximated by $S_3/T = 140$.
- Percolation temperature T_p: the temperature when dominant gravitational wave is generated. It is defined by the false vacuum fraction $P(T_p) \approx 0.7$, where

$$P(T) \equiv \mathrm{e}^{-I(T)}\,, \quad I(T) \equiv \frac{4\pi}{3}\int_T^{T_c} \mathrm{d}T' \frac{\Gamma(T')v_w^3}{T'^4 H(T')}\left[\int_T^{T'} \frac{\mathrm{d}T''}{H(T'')}\right]^3 .$$

Supercooling gravitational wave

- A supercooled phase transition occurs when the transition happens at temperature T_* much lower than critical temperature $T_*/T_c \ll 1$ [Guth 1980, and many].
- The high-temperature phase transition is generally assumed to be quick such that $T_p \approx T_n$, whereas the supercooled phase transition is long-lasting and possesses a much later bubble collision, resulting in $T_p \ll T_n$.
- T_p can be as low as a few MeV, while most of the true vacuum bubbles are nucleated around GeV. The gravitational wave is mainly produced by the collisions of large bubbles, featuring a suppressed transition rate but a large signal amplitude, with peak frequency as low as $f \sim 10^{-9} - 10^{-7}$ Hz, which is compatible with the pulsar timing array (PTA) experiments.

The commonly used effective potential for GW analysis

For a simple $U(1)_x$ model,

$$\mathcal{L} = -\frac{1}{4}F_{\mu\nu}F^{\mu\nu} + \left|(\partial_\mu - igA_\mu)\Phi\right|^2 - V_{\text{eff}}\,,$$

the temperature dependant effective action reads

$$V_{\text{eff}} = V_0(\Phi) + V_0^{1-\text{loop}}(\phi) + V_T^{1-\text{loop}}(\phi, T) + V_{\text{daisy}}(\phi, T)\,.$$

With the gauge fixing term and ghost Lagrangian, the field dependent masses are

$$\begin{aligned} m_A^2 &= g^2\phi^2\,, \\ m_h^2 &= -\mu^2 + 3\lambda\phi^2\,, \\ m_c^2 &= \xi m_A^2\,, \\ m_G^2 &= (-\mu^2 + \lambda\phi^2) + \xi m_A^2\,. \end{aligned}$$

Nielsen identity

The R_ξ gauge dependence of the effective action is described by [Nielsen, 1975] identity

$$\xi \frac{\partial S_{\text{eff}}}{\partial \xi} = -\int \mathrm{d}^4 x \, \frac{\delta S_{\text{eff}}}{\delta \phi(x)} \, C(x) \,,$$
$$C(x) = \frac{ig}{2} \int \mathrm{d}^4 y \Big\langle \bar{c}(x) G(x) c(y) \times \left[\partial_\mu A^\mu(y) + \sqrt{2} \xi g \phi G(y) \right] \Big\rangle \,.$$

Performing a gradient expansion of S_{eff}, $C(x)$ and $\delta S_{\text{eff}}/\delta\phi$ in the power of derivatives of the background field ϕ [Metaxas, Weinberg, 1995][Garnya, Konstandina, 2012][Löfgren, Ramsey-Musolf, Schicho, Tenkanen, 2021; w/Hirvonena, 2022]

$$S_{\text{eff}} = \int \mathrm{d}^4 x \Big[V_{\text{eff}}(\phi) + \frac{1}{2} Z(\phi) \big(\partial_\mu \phi\big)^2 \Big] \,,$$
$$C(x) = C_0(\phi) + D(\phi) \big(\partial_\mu \phi\big)^2 - \partial^\mu \big[\tilde{D}(\phi) \partial_\mu \phi \big] + \mathcal{O}\big(\partial^4\big) \,,$$
$$\frac{\delta S_{\text{eff}}}{\delta \phi(x)} = \frac{\partial V_{\text{eff}}(\phi)}{\partial \phi} + \frac{1}{2} \frac{\partial Z}{\partial \phi} \big(\partial_\mu \phi\big)^2 - \partial^\mu \big[Z(\phi) \partial_\mu \phi \big] + \mathcal{O}\big(\partial^4\big) \,.$$

Expansion matching

To employ the power counting, the effective potential $V_{\rm eff}$ and renormalization factor Z are expanded with respect to the gauge coupling as

$$\begin{aligned} V_{\rm eff} &= V(g^{\rm LO}) + V(g^{\rm NLO}) + \mathcal{O}(g^{\rm higher})\,, \\ Z &= 1 + Z_{g^2} + \mathcal{O}(g^4)\,, \\ C_0 &= C_{g^2} + C_{g^4} + \mathcal{O}(g^6)\,, \\ D, \tilde{D} &= 1 + \mathcal{O}(g^2)\,. \end{aligned}$$

The leading and sub-leading order contributions of Nielsen identity are

$$\begin{aligned} \xi \frac{\partial V_{g^4}}{\partial \xi} &= 0\,, \\ \xi \frac{\partial V_{g^6}}{\partial \xi} &= -C_{g^2} \frac{\partial V_{g^4}}{\partial \phi}\,, \\ \xi \frac{\partial Z_{g^2}}{\partial \xi} &= -2 \frac{\partial C_{g^2}}{\partial \phi}\,. \end{aligned}$$

Power counting

To employ the power counting, the effective potential $V_{\rm eff}$ and renormalization factor Z are expanded with respect to the gauge coupling as

$$\begin{aligned}
\text{High } T: \quad & V_{\rm eff} = V_{g^3} + V_{g^4} + \mathcal{O}(g^5)\,, && [1205.3392; 2112.05472; 2112.08912] \\
\text{Low } T: \quad & V_{\rm eff} = V_{g^4} + V_{g^6} + \mathcal{O}(g^8)\,, && [9507381; \text{WZF, Jinzheng Li, Nath, Ye, 2025}] \\
& Z = 1 + Z_{g^2} + \mathcal{O}(g^4)\,, \\
& C_0 = C_{g^2} + C_{g^4} + \mathcal{O}(g^6)\,.
\end{aligned}$$

The leading and sub-leading order contributions of Nielsen identity are

$$\begin{aligned}
\xi \frac{\partial V_{g^4}}{\partial \xi} &= 0\,, \\
\xi \frac{\partial V_{g^6}}{\partial \xi} &= -C_{g^2} \frac{\partial V_{g^4}}{\partial \phi}\,, \\
\xi \frac{\partial Z_{g^2}}{\partial \xi} &= -2 \frac{\partial C_{g^2}}{\partial \phi}\,.
\end{aligned}$$

Power counting

High T analysis:

$$\begin{aligned} V_{\rm eff}(\phi,T) =& V_0 + V_{\rm ct} + V_{\rm CW} + V_T^{1-\rm loop} + V_{\rm daisy} \\ =& -\tfrac{1}{2}(\mu^2+\delta\mu^2)\phi^2 + \tfrac{1}{4}(\lambda+\delta\lambda)\phi^4 + F(m_h^2) + 3F(m_A^2) + F(m_G^2) - F(m_c^2) \\ &+ \tfrac{T^4}{2\pi^2}\left[J_B\big(\tfrac{m_h^2}{T^2}\big) + 3J_B\big(\tfrac{m_A^2}{T^2}\big) + J_B\big(\tfrac{m_G^2}{T^2}\big) - J_B\big(\tfrac{m_c^2}{T^2}\big)\right] \\ &- \tfrac{T}{12\pi}\left[\big(m_{A_L}^2+\Pi_{A_L}\big)^{3/2} - m_{A_L}^3 + \big(m_h^2+\Pi_h\big)^{3/2} - m_h^3\right], \end{aligned}$$

where

$$F(m_i^2) = \tfrac{m_i^4}{64\pi^2}\big(\log\tfrac{m_i^2}{\Lambda^2} - C_i\big)\,.$$

Using the expansion of J_B, one gets the leading contribution

$$\begin{aligned} V_{\rm LO} =& -\frac{\mu^2}{2}\phi^2 + \frac{\lambda}{4}\phi^4 + \frac{T^2}{24}\big(m_h^2 + 3m_A^2 + m_G^2 - m_c^2\big) + \cdots \\ =& -\frac{1}{2}\mu_{\rm eff}^2\,\phi^2 + \frac{\lambda}{4}\phi^4 + \cdots\,. \end{aligned}$$

Basic counting strategy for High T

The Higgs effective mass reads

$$-\mu_{\rm eff}^2 = -\mu^2 + \Big(\frac{1}{3}\lambda + \frac{1}{4}g^2\Big)T^2 \sim \mathcal{O}(g^3)\,, \qquad \text{at } T_n$$

and thus one takes $\lambda \sim g^3$. The numerical analysis shows the nucleation temperature T_n is just slightly below T_c, and thus one further takes

$$T \sim \phi\,.$$

By doing the power counting, one rearrange the effective potential to calculate the nucleation rate using $S_{\rm eff} = S_0 + S_1$

$$S_0 = \frac{1}{T}\int \mathrm{d}^3x \Big[V_{g^3}(\phi_b) + \frac{1}{2}\big(\partial_i\phi_b\big)^2\Big]\,,$$
$$S_1 = \frac{1}{T}\int \mathrm{d}^3x \Big[V_{g^4}(\phi_b) + \frac{1}{2}Z_g\big(\partial_i\phi_b\big)^2\Big]\,,$$

where B_0 is explicitly ξ-independent and by using the Nielsen identity, $\xi\frac{\partial B_1}{\partial \xi} = 0$.

In practice, however...

- Various arguments have been advanced against counting λ higher than $\mathcal{O}(g^4)$, which appears unconvincing (at least to me). We find that only the scaling $\lambda \sim \mathcal{O}(g^3)$ can result in a gauge-invariant result.
- Indeed, the pioneering work [Arnold, Espinosa, 1995] claimed that one should work in the regime $g^4 \ll \lambda \ll g^3$. However, in reality

In practice, however...

- Various arguments have been advanced against counting λ higher than $\mathcal{O}(g^4)$, which appears unconvincing (at least to me). We find that only the scaling $\lambda \sim \mathcal{O}(g^3)$ can result in a gauge-invariant result.
- Indeed, the pioneering work [Arnold, Espinosa, 1995] claimed that one should work in the regime $g^4 \ll \lambda \ll g^3$. However, in reality
  1. To achieve detectable GW signals, (1) the hidden-sector gauge coupling g should not be small, hence higher powers of g does not offer a desirable suppression. (2) the Higgs quartic coupling λ is forced to be small, sometimes well below $\mathcal{O}(g^4)$.

In practice, however...

- Various arguments have been advanced against counting λ higher than $\mathcal{O}(g^4)$, which appears unconvincing (at least to me). We find that only the scaling $\lambda \sim \mathcal{O}(g^3)$ can result in a gauge-invariant result.
- Indeed, the pioneering work [Arnold, Espinosa, 1995] claimed that one should work in the regime $g^4 \ll \lambda \ll g^3$. However, in reality
  1. To achieve detectable GW signals, (1) the hidden-sector gauge coupling g should not be small, hence higher powers of g does not offer a desirable suppression. (2) the Higgs quartic coupling λ is forced to be small, sometimes well below $\mathcal{O}(g^4)$.
  2. For the case of SM at the electroweak scale, $g_Y \sim 0.3, g_2 \sim 0.6$, and the Higgs quartic coupling $\lambda_H \sim 0.1$. The counting $g^4 \ll \lambda \ll g^3$ is not satisfied to begin with.

In practice, however...

- Various arguments have been advanced against counting λ higher than $\mathcal{O}(g^4)$, which appears unconvincing (at least to me). We find that only the scaling $\lambda \sim \mathcal{O}(g^3)$ can result in a gauge-invariant result.
- Indeed, the pioneering work [Arnold, Espinosa, 1995] claimed that one should work in the regime $g^4 \ll \lambda \ll g^3$. However, in reality
  1. To achieve detectable GW signals, (1) the hidden-sector gauge coupling g should not be small, hence higher powers of g does not offer a desirable suppression. (2) the Higgs quartic coupling λ is forced to be small, sometimes well below $\mathcal{O}(g^4)$.
  2. For the case of SM at the electroweak scale, $g_Y \sim 0.3, g_2 \sim 0.6$, and the Higgs quartic coupling $\lambda_H \sim 0.1$. The counting $g^4 \ll \lambda \ll g^3$ is not satisfied to begin with.
  3. Nevertheless, our analysis shows that the gauge invariant result does hold in the large g and small λ regime.

In practice, however...

- Various arguments have been advanced against counting λ higher than $\mathcal{O}(g^4)$, which appears unconvincing (at least to me). We find that only the scaling $\lambda \sim \mathcal{O}(g^3)$ can result in a gauge-invariant result.
- Indeed, the pioneering work [Arnold, Espinosa, 1995] claimed that one should work in the regime $g^4 \ll \lambda \ll g^3$. However, in reality
  1. To achieve detectable GW signals, (1) the hidden-sector gauge coupling g should not be small, hence higher powers of g does not offer a desirable suppression. (2) the Higgs quartic coupling λ is forced to be small, sometimes well below $\mathcal{O}(g^4)$.
  2. For the case of SM at the electroweak scale, $g_Y \sim 0.3, g_2 \sim 0.6$, and the Higgs quartic coupling $\lambda_H \sim 0.1$. The counting $g^4 \ll \lambda \ll g^3$ is not satisfied to begin with.
  3. Nevertheless, our analysis shows that the gauge invariant result does hold in the large g and small λ regime. So what's the point of the counting?
- The higher g power gauge-dependent terms dropped might be problematic, e.g.,

$$F(m_G^2) - F(m_c^2) \simeq F'(m_c^2)\,(m_G^2 - m_c^2) \sim \xi\mathcal{O}(g^5)\,.$$

Modification to the zero temperature results

For the supercooled phase transition $T \ll M$, one expects $T_* \to 0$, and one expects the temperature dependent term $\delta Z_{g_x^2}(\phi, T)$ only offers little contribution

$$Z(\phi) = 1 + Z_{g_x^2}(\phi, T=0) + \delta Z_{g_x^2}(\phi, T) + \mathcal{O}(g_x^4)\,,$$

where the zero-temperature factor $Z_{g_x^2}(\phi, T=0)$

$$Z_{g_x^2}(\phi, T=0) = \frac{g_x^2}{16\pi^2}\left[\xi \ln\left(\frac{2g_x^2\phi^2\xi}{\Lambda^2}\right) + 3\ln\left(\frac{2g_x^2\phi^2}{\Lambda^2}\right) + \xi\right].$$

For the low T power counting, we use [WZF, Jinzheng Li, Nath, Ye, 2025]

$$\lambda \lesssim \mathcal{O}(g^4)\,, \qquad T \lesssim \mathcal{O}(g\phi)\,. \tag{1}$$

Expansion matching

We find in the low temperature regime,

$$
\begin{aligned}
S_{\text{eff}} &= S_0 + S_1 \,, \\
S_0 &= \beta \int \mathrm{d}^3 x \left[\frac{1}{2} (\partial_\mu \phi_b)^2 + V_{g_x^4}(\phi_b) \right] \,, \\
S_1 &= \beta \int \mathrm{d}^3 x \left[\frac{1}{2} Z_{g_x^2}(\phi_b, \xi) (\partial_\mu \phi_b)^2 + V_{g_x^6}(\phi_b, \xi) \right] \,.
\end{aligned}
$$

Comparing with the gauge-dependent result

$$
S_{\text{eff}}^{\text{G.D.}} = \beta \int \mathrm{d}x^3 \left[\frac{1}{2} (\partial_\mu \phi)^2 + V_{\text{eff}}(\phi, \xi) \right] \,,
$$

Results: gauge-independent vs gauge-dependent

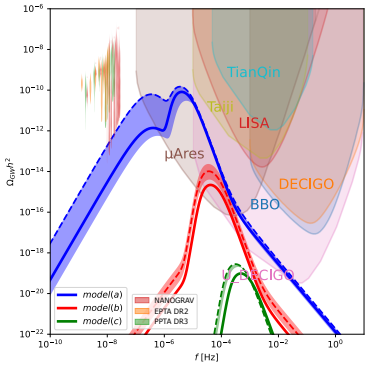

Figure: Analysis of gravitational wave power spectra for model configurations (a), (b), and (c) which shows variations in parameter ξ across the range $(-1, 1)$. The solid line displays the gauge-invariant solution. The dashed line displays the Landau gauge solution.

Sub-GeV supercooled phase transition

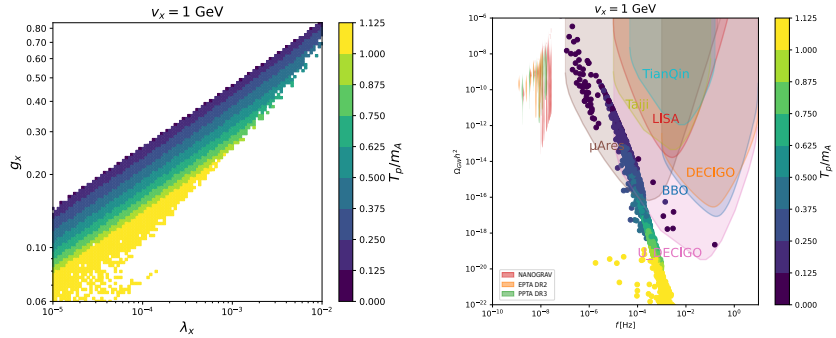

Figure: Left panel: Parameter scan within the $g_x - \lambda_x$ parameter plane, with v_x fixed at 1 GeV. Right panel: Theoretical predictions for gravitational wave power spectra corresponding to the parameter configurations displayed in the upper panel. Each point marks the peak of the power spectrum. The color coding indicates the ratio $T_p/m_{\gamma'_x}$.

$U(1)_x$ phase transition: Sub-GeV – EW

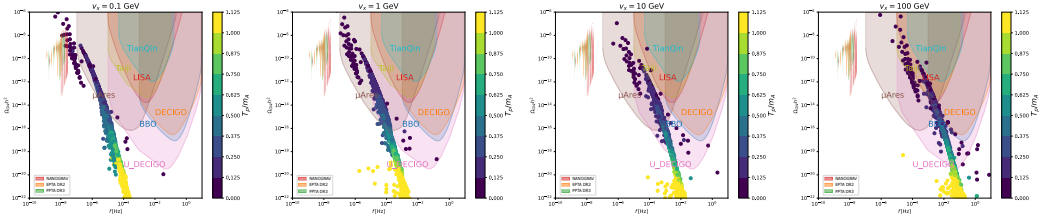

Figure: Predictions for gravitational wave power spectra with the same parameter scan range by gauge-invariant analysis. Each point marks the peak of the power spectrum. The color coding indicates the ratio $T_p/m_{\gamma'_x}$. Different vevs are chosen here ($v_x = 0.1, 1, 10, 100$GeV).

Is S_1 really subleading?

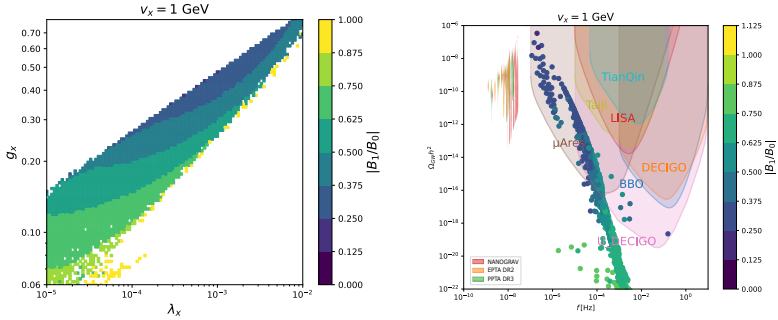

Figure: Left Panel: Ratio $|S_1/S_0|$ at T_p across (g_x, λ_x) with $v_x = 1$ GeV. Right Panel: Correlation between gravitational-wave spectra and $|S_1/S_0|$ at $v_x = 1$ GeV. Models with the largest GW peak amplitudes, which offer detectable GW signals, preferentially exhibit smaller $|S_1/S_0|$, indicating the perturbative control is strongest in the phenomenologically most relevant regions.

Conclusion and discussions

- A $B - L$ conserving Universe with $\mathcal{O}(1\ \text{GeV})$ dark matter candidates can simultaneously account for: the baryon asymmetry, the nature of dark matter, the observed dark-to-baryon abundance ratio, and neutrino masses and mixings.
- This framework is testable via multi-messenger searches: GW observations of FOPT, laboratory probes of sub-GeV dark photons with small kinetic mixing, direct detection of $\mathcal{O}(\text{GeV})$ asymmetric dark matter, and cosmological tests of neutrino properties and non-unitarity associated with the extended fermion sector.
- We demonstrate that gauge-invariant analysis is relevant for reliable predictions for the gravitational wave backgrounds and in general gravitational wave power spectrum is sensitively dependent of gauge choice.
- Our GW analysis applies broadly to all $U(1)_x$ hidden sector phase transitions occurring at sub-GeV – EW scale.

Open questions for the gauge invariant approach:

- What's the point of the power counting?
- Bottom line of the methodology.
- Can we do better? and what shall we do further?